Torsion-Sensing Material from Aligned Carbon Nanotubes Wound onto a Rod Demonstrating Wide Dynamic Range

Takeo Yamada,[†] Yuki Yamamoto,[†] Yuhei Hayamizu,[†] Atsuko Sekiguchi,[†] Hiroyuki Tanaka,[†] Kazufumi Kobashi,[†] Don N. Futaba,[†] and Kenji Hata[†,‡,*]

[†]Nanotube Research Center, National Institute of Advanced Industrial Science and Technology (AIST), Tsukuba, 305-8565, Japan and [‡]Japan Science and Technology Agency (JST), Kawaguchi 332-0012, Japan

ABSTRACT A rational torsion sensing material was fabricated by wrapping aligned single-walled carbon nanotube (SWCNT) thin films onto the surface of a rod with a predetermined and fixed wrapping angle without destroying the internal network of the SWCNTs within the film. When applied as a torsion sensor, torsion could be measured up to 400 rad/meter, that is, more than 4 times higher than conventional optical fiber torsion sensors, by monitoring increases in resistance due to fracturing of the aligned SWCNT thin films.

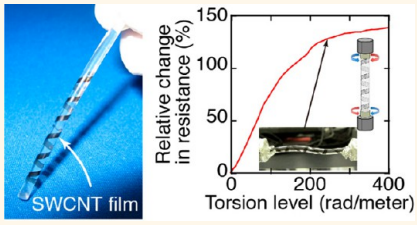

KEYWORDS: single-walled carbon nanotube · torsion sensor · transfer · torsion level · strain

Deformation describes the distortion of an object from applied forces, which can result in stretching, compressing, shearing, twisting, vibration, torsion, and bending. Sensing these deformations is important to monitor the complex motion and position of objects, such as human motion. The most well-known deformation sensor is the strain gauge that operates by registering changes in electrical properties, *e.g.*, resistance, when subjected to strain. From this basic sensor, acceleration, pressure, tension, and strain can be monitored on an object, and these gauges have been used in cars, airplanes, building, and bridges.

Torsion is strain about an axis and represents a significantly more complex deformation than linear strain. Torsion is commonly observed in the motion of natural muscles, robotics, and even torsional carbon nanotube artificial muscles.[1] In contrast to linear strain, the surface of a torsionally strained object undergoes both linear and rotational strain; hence, the object experiences shearing at the surface. The complexity of this strain has limited the development of simple torsion-sensing materials, and existing sensors are built on complicated systems using optical fiber devices with Bragg gratings (FBG)[2,3] and corrugated long-period fiber gratings (LPFG).[4−6] For example, for the FBG torsion sensor, when the optical fiber is torsionally strained, the strain components induce strain along the fiber axis and therefore a shift in Bragg wavelength within the FBG. The amount of torsion is then determined by detecting the shift in the Bragg wavelength.[2,3]

Recently, the emerging new paradigms for electronics with the attributes of flexibility and stretchability to realize soft and human-friendly devices have driven the development of new stretchable and conductive materials. Apt examples include polymer composites with conductive fillers[7−9] and extremely thin metal films on stretchable polymer substrates.[10] Stretchable, yet conductive, materials offer an opportunity to measure the strain-dependent change in electronic performance to monitor deformation. Such new materials with superior tolerances against high levels of strain might serve as sensors with more robust properties and wider dynamic sensing ranges than, for example, a conventional strain gauge consisting of unstretchable metal thin films. For example, it was found that aligned single-walled carbon nanotube (SWCNT) thin films could deform when stretched in a manner similar to the structural deformation of peeled string cheese and thus withstand strains up to 280%,[11] a value markedly higher than the 5% limit of conventional metal strain gauges described

* Address correspondence to kenji-hata@aist.go.jp.

Received for review December 3, 2012 and accepted March 6, 2013.

Published online March 06, 2013
10.1021/nn305593k

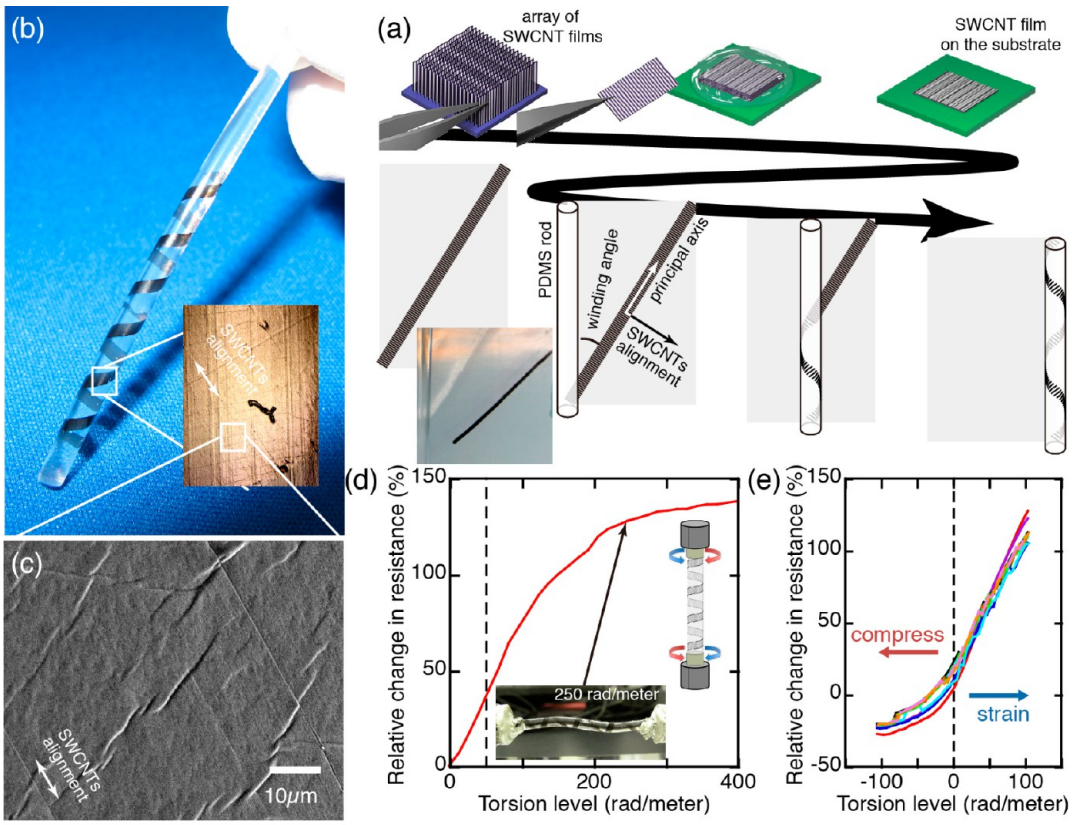

Figure 1. (a) Process steps in fabricating the SWCNT film torsion-sensing material and array of thin SWCNT films grown. One film was picked up and laid down on the substrate densfied by solution and dried. (b) Photograph of the SWCNT film torsion-sensing material. Inset: Optical microscope image of the SWCNT film on the elastomeric rod. (c) Scanning electron microscope (SEM) image of the SWCNT film on the elastomeric rod. (d) Relative change in resistance *versus* torsion rate. Inset: Image of SWCNT film torsion sensor and photograph of the SWCNT film torsion sensor at a torsion level of 250 rad/meter. (e) Relative change in resistance *versus* torsion level repeated for 1000 torsion cycles of ±100 rad/meter.

above. A strain sensor assembled from this SWCNT thin film measured strain with high durability (10 000 cycles at 150% strain), fast response (delay time: 14 ms), and low creep (3.0% at 100% strain). Moreover, the strain sensor could precisely monitor rapid, large-scale human motion by embedding the strain sensors into clothing to detect movement, typing, breathing, and phonation (speech).[11]

In this article, a rational rod torsion-sensing material was demonstrated that could be used as a sensor to measure torsion (400 rad/meter) more than 4 times higher than conventional optical fiber torsion sensors[6] by monitoring increases in resistance due to fracturing of an aligned SWCNT thin film wrapped around a rod. The exceptionally large torsion tolerance of the torsion sensor originated from the large stain tolerance (up to 280%) of the SWCNT thin film[11] that was wrapped around the rod with a predetermined angle to optimally align the principle axis of the SWCNT film with the direction of the torsional strain.

RESULTS AND DISCUSSION

Representative resistivity–torsion data recorded for the sensor in Figure 1d showed a linear increase up to 50 rad/meter and a monotonic and continuous increase up to 400 rad/meter. In other torsion sensors (Figure 1d), a linear increase of resistance up to 200 rad/meter is observed, pointing to the possibility to even further increase the range of linearity by structural optimization This monotonic increase in resistivity with torsion demonstrated the potential use of this device as a gauge to measure large torsion much higher than the 30 rad/meter limit of LPFG[5] and the 100 rad/meter limit of rotary-LPFG.[6] When torsion was applied in the opposite direction, the resistivity decreased (Figure 1e), demonstrating the ability to discriminate between left- and right-handed twists. However, the resistivity–torsion behavior for left-handed torsional strain was less sensitive and less linear. When the torsion level exceeded 100 rad/meter, the torsion sensor failed from buckling and lifting of the SWCNT thin film. In the opposite direction, buckling and lifting occurred much more easily, resulting in nonlinear behavior of electrical resistance with a small torsion level. The inability to measure bidirectional torsion is one of weaknesses of this current torsion sensor. One possible approach to overcome this issue is to wind SWCNT thin films on a prestrained PDMS rod.

Our SWCNT torsion sensor exhibited reasonable durability. Fatigue testing of the sensor for 1000 torsion

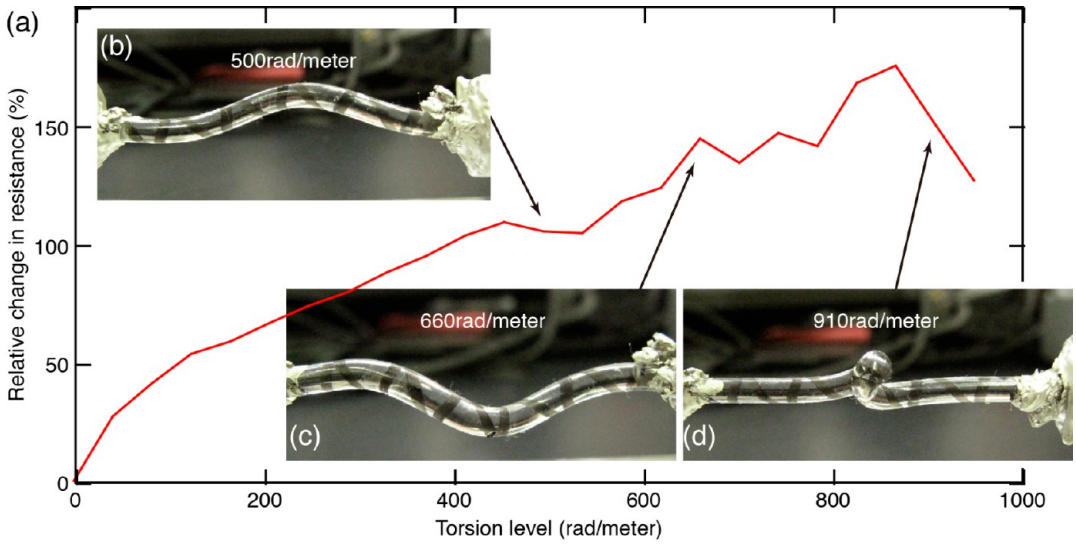

Figure 2. (a) Relative change in resistance *versus* torsion level up to 950 rad/meter. (b–d) Photographs of the SWCNT film torsion sensor at torsion levels of 500, 660, and 910 rad/meter, respectively.

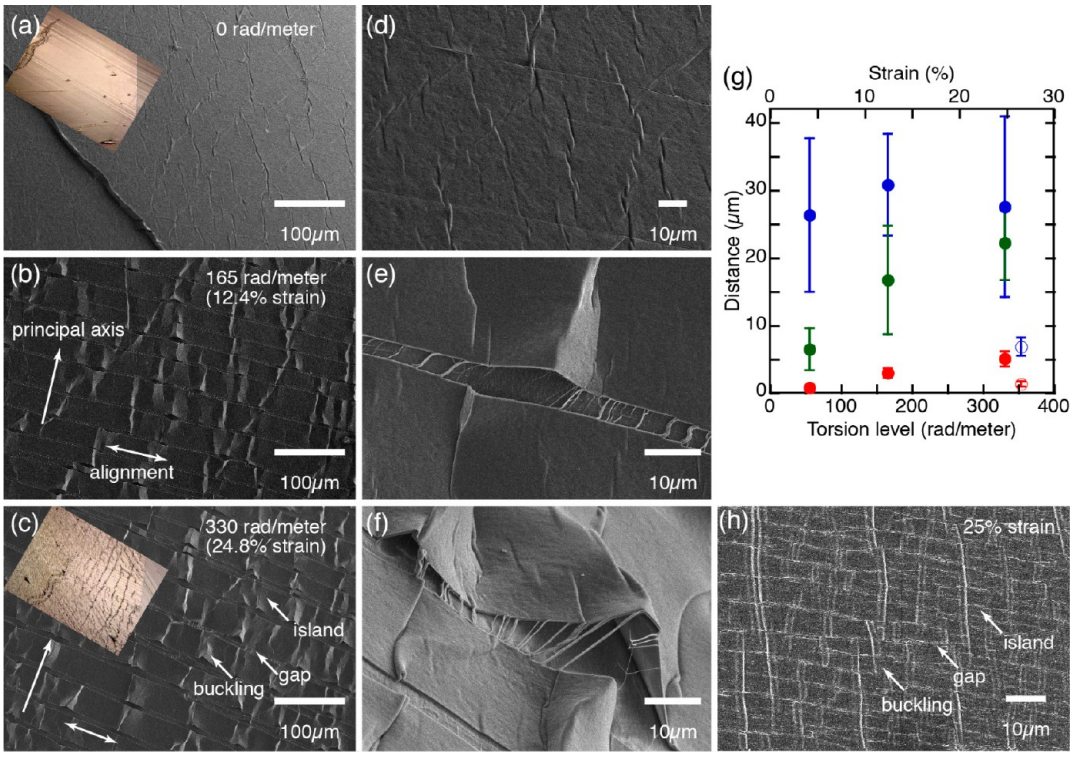

Figure 3. (a–c) Low-resolution SEM images of the SWCNT film at 0 (a), 165 (b), and 330 (c) rad/meter torsion with 45° winding angle. Inset of (a) and (c): Optical microscope image of the SWCNT film at 0 (a) and 330 (c) rad/meter twist. (d–f) High-resolution SEM images of the SWCNT film at 0 (d), 165 (e), and 330 (f) rad/meter torsion with 45° winding angle. (g) Average island width (solid blue circle), gap (solid red circle), and buckling size (solid green circle) *versus* torsion level and strain for initial loading of the torsion sensor with 45° winding angle. Open blue and red circles indicate island width and gap size, respectively, for the linear CNT strain sensor at ~25% strain. (h) SEM image of the fracturing of the SWCNT film of the linear strain sensor at 25% strain.

cycles of ±100 rad/meter showed that the electrical response remained fairly unchanged (Figure 1e).

Intrinsically our torsion sensor could bear torsion much higher than 400 rad/meter, as demonstrated by the resistivity–torsion data shown up to 950 rad/meter (Figure 2a). First, the ability to record resistivity data throughout this torsion range meant that the SWCNT film sensing material could withstand this high level of torsion without being ruptured. Second, beyond 400 rad/meter, in general, the resistance followed the

increasing trend with torsion; however, local variations arose. Pictures of the torsion sensor at different torsion levels showed various levels of rod buckling due to stress concentration on the polymeric rod (Figure 2b–d). It is interpreted that this nonuniform buckling led to nonuniform strain on the film surface and therefore to the local variations in the measured resistance. Hence, this limited the sensing range of the device. This meant that the device measurement range was governed by the elastomeric properties of the rod rather than the SWCNT thin film, and thus further improvement could be expected by tailoring the material and radius of the rod to prevent strain-induced buckling.

To understand the underlying mechanism of the torsion-sensing material, the structural change in the SWCNT film was examined under different levels of torsion. Initial application of torsion resulted in fracturing throughout the SWCNT film, which created islands, gaps, and surface buckling of the SWCNT film surface. Upon further torsion, the width of the gaps and surface buckling increased (Figure 3a–f). Importantly, suspended SWCNT bundles bridging the gaps (an appearance similar to peeled string cheese) were created and prevented complete film rupture. Film fracture led to an increase in resistance, explaining the observed linear resistivity behavior. SWCNT bundles bridging the gaps are the unique feature of the aligned SWCNT film that allowed exceptional torsion tolerance. Lateral interconnections between the SWCNTs were essential to create the suspended bundles, and millimeter-scale SWCNTs produced durable and elongated bundles spanning wide gaps. The islands, in contrast, acted as anchors to prevent film detachment from the rod substrate. Furthermore, in the direction parallel to the principle axis, surface shear forces induced extensive film buckling (Figure 3f) that increased with torsion level.

The observed fracturing greatly differed from the same aligned SWCNT film when applied as a linear strain sensor, *i.e.*, when stretched linearly along the principle axis.[11] Although, the fundamental features of fracturing, *i.e.*, islands, gaps, and bridges, and surface-buckling were observed for both sensors, the representative scale of each feature and the response to the deformation were different. In general, when acting as a torsion sensor, the SWCNT film fractured into much larger segments, as demonstrated by the 4, 7, and 15 times larger width of the gaps, islands, and level of SWCNT buckling compared to that of the linear SWCNT strain sensors. The difference lies in the fracturing properties when additional strain (torsion) was applied. Further, unlike the linear strain sensors, where strain in the SWCNT film resulted in island fragmentation into smaller islands and increased gap separation (Figure 3g), strain in the SWCNT film for torsion sensor was observed by SWCNT film buckling and increased gap separation. The SWCNT film buckling was the particularly prominent difference for the torsion sensor, as it was not

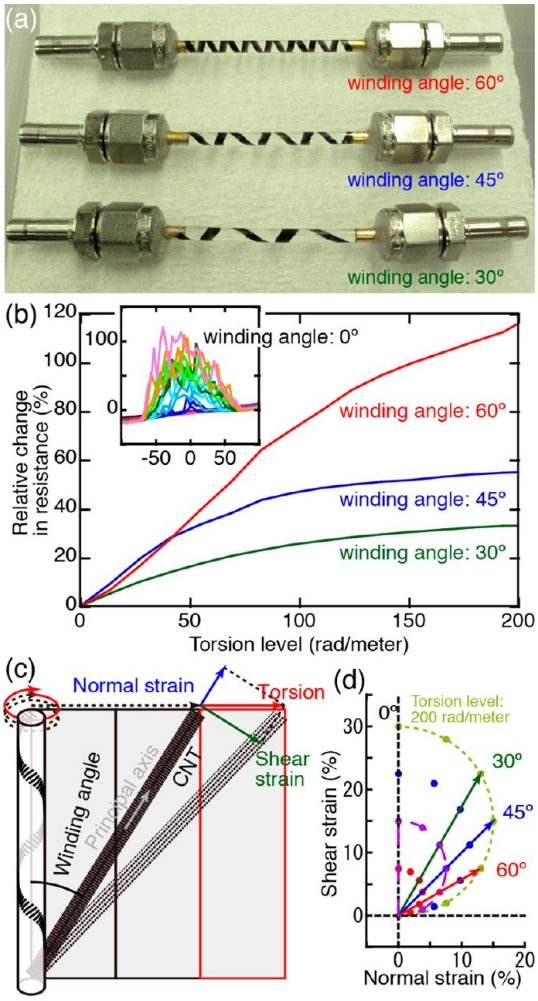

Figure 4. (a) Photograph of the SWCNT film torsion-sensing material with 30°, 45°, and 60° winding angles. (b) Relative changes in resistance *versus* torsion level for the SWCNT film torsion sensors with 30° (green), 45° (blue), and 60° (red) winding angles. Inset: Relative changes in resistance *versus* 100 to −100 rad/meter torsion cycles for the torsion sensor with 0° winding angle. (c) Schematic of the torsion sensor strain. (d) Normal and shear strain vectors invoked by the torsional action (purple and light green dotted half circle lines show 100 and 200 rad/meter torsion level, respectively) and with respect to 30° (green vector), 45° (blue vector), and 60° (red vector) winding angle.

observed for the linear SWCNT strain sensor (Figure 3h). It is interpreted that, once this buckling occurred, it prevented the film from fracturing into smaller segments. When torsion was applied, the SWCNT film experienced not only normal strain along the principal axis but also shear strain in the perpendicular direction. It is interpreted that this shear strain induced the extensive buckling and meant that the shearing forces were destructive to the SWCNT torsion sensor. It should also be noted that the sensing mechanism of the torsion sensor provides selectivity against bending. This is because torsion acts on the entire SWCNT thin film, while bending acts locally on a section of the SWCNT thin film, thus giving a relatively small change in the resistivity.

The winding angle of the SWCNT film of the rod was an important parameter that governed the ratio between normal and shear strain when torsion was applied. The importance of the winding angle was readily demonstrated by the failure of a SWCNT film with 0 winding angle (along the principle axis) to gauge the torsion because the resistivity showed a chaotic change of resistance with increased torsion in contrast to a monotonic increase (Figure 4b, inset). Therefore, the effect of winding angle on the performance of the torsion sensors was investigated by fabricating three torsion sensors with different SWCNT film winding angles (30°, 45°, and 60°) (Figure 4a) and torsion-resistance behavior (Figure 4b). As shown in Figure 4b, the increase in sensitivity (gauge factor) of the torsion sensor as well as the 225% linear increase with the winding angle demonstrated the preference of larger winding angles. A schematic of the torsion sensor is presented to illustrate the normal and shear strain vectors acting on SWCNT films, with respect to the principal axis, wrapped on a rod with predetermined winding angles at different torsional strain (Figure 4c). Normal/shear strain is defined as the component parallel/perpendicular to the principal axis. It is important to note that the magnitude of the normal strain vector determined the sensitivity of the torsion sensor, while that of the (destructive) shear vector governed the torsion tolerance. A two-dimensional map was constructed from the schematic to show the dependence of the magnitudes of the strain *versus* torsion vectors on the torsion level and winding angle (Figure 4d). The map showed that the shear strain decreased with increasing winding angle; thus a larger winding angle was preferred to minimize the destructive shear strain, in agreement with experimental observation. However, above 45°, the normal strain also decreased with increasing winding angle, which resulted in a decrease in sensitivity of the torsion sensor. It should be noted that this is in agreement with standard solid mechanics theory for the surface stress distribution on a solid rod from torsion where the maximum shear stress occurs at 45° with respect to the long axis. As such, the winding angle must be chosen to balance sensitivity (large normal strain vector) and torsion tolerance (small shear strain vector). Our experimental results found a winding angle of 60° to be optimal, as the sensitivity (proportional to the magnitude of the normal strain vector) was similar to that at 30° and 87% smaller than that at 45°, while the torsion tolerance (proportional to the magnitude of the shear strain vector) was one-third of that at 30°.

SUMMARY

In conclusion, a torsion-sensing material composed of an aligned SWCNT thin film embedded on the surface of an elastomeric ϕ 3 mm rod that could be applied as a sensor to measure a very large torsion level of 400 rad/meter, 4 times higher than conventional optical fiber sensors, was demonstrated.[2−6] The torsion sensor has several advantages over conventional torsion sensors that use optical fibers. The device was simpler and could be made very small, and thus the sensor could be easily surface mounted or directly embedded in many components subjected to torsional motion. The aligned SWCNT films as used in this research have also shown low creep and fast response on the order of milliseconds.[11] In principle, any form of aligned CNTs would likely be useable as a strain and torsion sensor; therefore multiwalled CNT (MWCNT) arrays drawn from a MWCNT forest might also be used, giving a simple route for mass production of these sensors.[16,17] Furthermore, the aligned SWCNT film demonstrated good signal-to-noise selectivity against environmental effects, such as temperature and humidity, through coating with polydimethylsiloxane (PDMS) without losing the ability to monitor strain. These features make our torsion sensor a promising tool to monitor motions and deformations of human, robots, and emerging new stretchable devices for applications in a wide range of fields, such as recreation, virtual reality, and health care.

EXPERIMENTAL METHOD

The key process in fabricating the torsion-sensing material was to wrap the aligned SWCNT thin film onto the surface of a rod with a predetermined and fixed wrapping angle without destroying the internal network of the SWCNTs within the film. This difficulty was magnified by the need to assemble the film onto a rod with a 10 cm length, while simultaneously accounting for the fragile film (thickness: 400 nm). To overcome these difficulties, first aligned SWCNT thin films were assembled onto a flat Teflon substrate and then simply rolling an elastomeric rod across the Teflon substrate at a predefined angle (Figure 1). The relatively weak adhesion force between the Teflon substrate and SWCNT film compared to that among the SWCNTs within the film and to that between the elastomeric rod and SWCNT film allowed efficient transfer of the entire SWCNT film onto the elastomeric rod with no residual SWCNTs remaining on the surface and minimal structural distortion to the thin film. SEM observation showed no significant damage to the SWCNT films from the transfer process. In general, transferring of SWCNT thin films without incurring structural damage is made fairly easy because of the mechanical cohesion within the SWCNT film stemming from the intertwining among the long SWCNTs. It is surmised that this is because the SWCNT thin film is a macroscopic assembly of very long and intertwined SWCNTs held together by their imperfect alignment. This intertwining provides a mechanical cohesion in the SWCNT thin films, making it easy to transfer while retaining the internal structure.

Figure 1a schematically illustrates the processes in fabricating the SWCNT film torsion-sensing material. Vertically aligned and very sparse (3−4% occupancy) SWCNT thin films (height, 1 mm; width, 6 mm; length, 16 mm) were first grown from lithographically patterned catalysts using water-assisted chemical vapor deposition.[12] Films were individually removed and laid side by side, with a 1 mm overlap,[11] onto a flat Teflon substrate with the alignment of the SWCNTs arranged perpendicular to the

principal axis. For each iteration, the film was wet with a droplet of isopropyl alcohol, which flattened the film (thickness: 400 nm) to the substrate in a manner similar to deflating an air mattress. This allowed the SWCNTs to be packed into a highly dense solid form (density, ~0.46 g/cm^3; occupancy, ~42%; SWCNT spacing, ~1.3 nm).[13,14] An elastomeric (PDMS) ϕ 3 mm rod was slowly rolled across the Teflon substrate along a predetermined direction relative to the principal axis of the SWCNT film. In this way, the SWCNT film was transferred to the elastomeric rod (Figure 1b and c). Finally, to fabricate the sensor, two electrodes were attached at both ends of the rod with either silver paste or a SWCNT conductive rubber paste.[11,15]

Conflict of Interest: The authors declare no competing financial interest.

Acknowledgment. The authors thank T. Toida for his assistance. The authors also acknowledge partial support from Core Research for Evolutional Science and Technology (CREST) of the Japan Science and Technology Agency (JST).

REFERENCES AND NOTES

1. Foroughi, J.; Spinks, G. M.; Wallace, G. G.; Jiyoung, O.; Kozlov, M. K.; Fang, S.; Mirfakhrai, T.; Madden, J. D. W.; Shin, M .K.; Kim, S. J.; *et al*. Torsional Carbon Nanotube Artificial Muscles. *Science* **2011**, *334*, 494–497.
2. Tian, X. G.; Tao, X. M. Torsion Measurement Using Fiber Bragg Grating Sensors. *Exp. Mech.* **2001**, *41*, 248–253.
3. Kruger, L.; Swart, P. L.; Chtcherbakov, A. A.; van Wyk, A. J. Non-Contact Torsion Sensor Using Fiber Bragg Gratings. *Meas. Sci. Technol.* **2004**, *15*, 1448–1452.
4. Wang, L. A.; Lin, C. Y.; Chern, G. W. A Torsion Sensor Made of a Corrugated Long Period Fiber Grating. *Meas. Sci. Technol.* **2001**, *12*, 793–799.
5. Rao, Y. J.; Zhu, T.; Mo, Q. J. Highly Sensitive Fiber-Optic Torsion Sensor Based on an Ultra-Long-Period Fiber Grating. *Opt. Commun.* **2006**, *266*, 187–190.
6. Shi, L.; Zhu, T.; Fan, Y.; Chiang, K. S.; Rao, Y. Torsion Sensing with a Fiber Ring Laser Incorporating a Pair of Rotary Long-Period Fiber Gratings. *Opt. Commun.* **2011**, *284*, 5299–5302.
7. Cochrane, C.; Koncar, V.; Lewandowski, M.; Dufour, C. Design and Development of a Flexible Strain Sensor for Textile Structures Based on a Conductive Polymer Composite. *Sensors* **2007**, *7*, 473–492.
8. Mattmann, C.; Clemens, F.; Tröster, G. Sensor for Measuring Strain in Textile. *Sensors* **2008**, *8*, 3719–3732.
9. Shin, M. K.; Jiyoung, O.; Lima, M.; Kozlov, M. E.; Kim, S. J.; Baughman, R. H. Elastomeric Conductive Composites Based on Carbon Nanotube Forests. *Adv. Mater.* **2010**, *22*, 2663–2667.
10. Lacour, S. P.; Chan, D.; Wagner, S.; Li, T.; Suo, Z. Mechanisms of Reversible Stretchability of Thin Metal Films on Elastomeric Substrates. *Appl. Phys. Lett.* **2006**, *88*, 204103.
11. Yamada, T.; Hayamizu, Y.; Yamamoto, Y.; Yomogida, Y.; Izadi-Najafabadi, A.; Futaba, D. N.; Hata, K. A Stretchable Carbon Nanotube Strain Sensor for Human-Motion Detection. *Nat. Nanotechnol.* **2011**, *6*, 296–301.
12. Hata, K.; Futaba, D. N.; Mizuno, K.; Namai, T.; Yumura, M.; Iijima, S. Water-Assisted Highly Efficient Synthesis of Impurity-Free Single-Walled Carbon Nanotubes. *Science* **2004**, *306*, 1362–1364.
13. Futaba, D. N.; Hata, K.; Yamada, T.; Hiraoka, T.; Hayamizu, Y.; Kakudate, Y.; Tanaike, O.; Hatori, H.; Yumura, M.; Iijima, S. Shape-Engineerable and Highly Densely Packed Single-Walled Carbon Nanotubes and Their Application as Super-Capacitor Electrodes. *Nat. Mater.* **2006**, *5*, 987–994.
14. Hayamizu, Y.; Yamada, T.; Mizuno, K.; Davis, R. C.; Futaba, D. N.; Yumura, M.; Hata, K. Integrated Three-Dimensional Microelectromechanical Devices from Processable Carbon Nanotube Wafers. *Nat. Nanotechnol.* **2008**, *3*, 289–294.
15. Sekitani, T.; Noguchi, Y.; Hata, K.; Fukushima, T.; Aida, T.; Someya, T. A Rubberlike Stretchable Active Matrix Using Elastic Conductors. *Science* **2008**, *321*, 1468–1472.
16. Zhang, M.; Fang, S.; Zakhidov, A. A.; Lee, S. B.; Aliev, A. E.; Williams, C. D.; Atkinson, K. R.; Baughman, R. H. Strong, Transparent, Multifunctional, Carbon Nanotube Sheets. *Science* **2005**, *309*, 1215–1219.
17. Jiang, K.; Qunqing, L.; Shoushan, F. Spinning Continuous Carbon Nanotube Yarns. *Nature* **2002**, *419*, 801–801.